ACCELERATED PAVEMENT TESTING FIRST RESULTS AT THE LANAMMEUCR APT FACILITY

Submitted to the 94th Annual Meeting of the Transportation Research Board
Submitted on July 22th, 2014

Fabricio Leiva-Villacorta, Ph.D., MBA, (corresponding author)
National Laboratory of Materials and Structural Models (LanammeUCR),
University of Costa Rica, P.O.Box 11501-2060, UCR, San José, Costa Rica
fabricio.leiva@ucr.ac.cr

José Pablo Aguiar-Moya, Ph.D.
National Laboratory of Materials and Structural Models (LanammeUCR)
University of Costa Rica, San José, Costa Rica
jose.aguiar@ucr.ac.cr

Luis Guillermo Loría-Salazar, Ph.D.
National Laboratory of Materials and Structural Models (LanammeUCR)
University of Costa Rica, San José, Costa Rica
luis.loriasalazar@ucr.ac.cr

Word Count: Abstract (249) + Body (3,960) + Figures and Tables (13x250) = 7,459

ABSTRACT

Traditionally, the design of pavements in Costa Rica has been made using the AASHTO 93 design method, which is related to empirical correlations of the results obtained several decades back in the AASHO road test. In order to return to the use of more fundamental engineering principles, the necessity of a transition from this empirical state to a mechanistic-empirical state has been recognized. The National Laboratory of Materials and Structural Models of the University of Costa Rica (LanammeUCR) has implemented a project as a starting point for this transition: the project involves characterization and engineering of improved materials, introduction of new technologies, improvement of existing specifications and the development of a pavement design guide specific for the country. With this in mind, LanammeUCR acquired a Heavy Vehicle Simulator (HVS) and started an Accelerated Pavement Testing (APT) program. Construction of the first test track sections was performed in May of 2012. These initial sections correspond to flexible and semi-rigid pavement structures and the experiment included: embedded instrumentation, non-destructive pavement evaluation and material characterization of all four test sections. The objective of this phase was to perform a structural comparison, in terms of thickness of the asphalt concrete layer and in terms of base material type (granular vs. cement treated). The effect of construction variability on pavement performance was a main concern for this study. Accelerated testing has finalized for one section. A description of the implemented APT program and results of the first experiment are also discussed in this document.

INTRODUCTION

Significant developments in pavement engineering have been traditionally achieved through real time load testing (RTL) because the technique does not require large specialized equipment for carrying out the tests (*1, 2*). However, the time required to perform the RLT tests (more than 10 years of continuous monitoring of an experimental section) is associated with many difficulties, since most of the experimental sections are located along roadways in operation.

In the case of Costa Rica, because of the large variability in climatic conditions, materials and traffic, the cost of developing a suitable RTL test program covering all these conditions for prolonged periods of time is prohibitive. However, there is a great need to characterize the performance of national pavement structures as the only means of developing and calibrating own design methodologies. For this purpose it was considered that the implementation of a Accelerated Pavement Testing (APT) program was a better alternative.

In order to implement a Costa Rican APT program, a technical and economical study was performed and aided in determining that the Heavy Vehicle Simulator (HVS) was the best fit for the medium and long term pavement performance assessment. Specifically, the HVS met the following requirements (*3, 4, 5*):

• Mobility: It can be used inside conditioned facilities or it can be easily driven out to the field.
• Accelerated Pavement Evaluation: It is able to simulate the deterioration of 20 years in a few months.
• Real loads: The number and location of loading applications can be controlled.
• Compatibility: the results generated can be compared to results from similar equipment and RLT tests.

APT program deliverables

The HVS will be essential to ensure a breakthrough in the level of research conducted by the LanammeUCR in transportation engineering. In particular, it is expected that a series of products that have already been obtained under similar studies (*6, 7, 8*) be generated:

- Mechanistic - empirical pavement design methodology and software based on material conditions, weather, traffic and actual construction practices.
- Development of new material specifications that are based on actual performance and contribution of structural materials in the field.

- Optimization of pavement structures in use at the national level, based on structural, materials, traffic, and climatic conditions specific to the area where the structure is planned to be built.
- Potential for an improved evaluation methodology of new materials or materials currently in use.
- Capacity to evaluate pavement structures of high importance prior to opening to traffic in order to ensure required performance of the structure or identify possible deficiencies.

TEST TRACKS

For the first stage of accelerated tests in Costa Rica the construction of 4 experimental sections was performed in May 2012 (Figure 1). The objective of this phase was to perform a structural comparison in terms of thickness of the asphalt concrete layer and base material type (granular vs. cement treated). Table 1 shows the characteristics of the 4 sections with their respective layer thicknesses obtained from Ground Penetrating Radar (GPR) measurements and backcalculated layer moduli based on Falling Weight Deflectometer results. The top layer consists of an HMA mixture with nominal maximum aggregate size of 19.0 mm with an optimum binder content of 4.9% by total weight of mixture. The cement treated base (CTB) was designed to withstand 35 kg/cm^2 with an optimum cement content of 1.7% by volume of aggregate and with a maximum density of 2013 kg/m^3. The base material and granular sub-base were placed at a maximum density of 2217 kg/m^3 with an optimum moisture content of 8.6%. The sub-base material had a CBR of 95%. Finally, the subgrade material was constructed for a maximum density of 1056 kg/m^3 with an optimum moisture content of 52% and CBR of 6.6%.

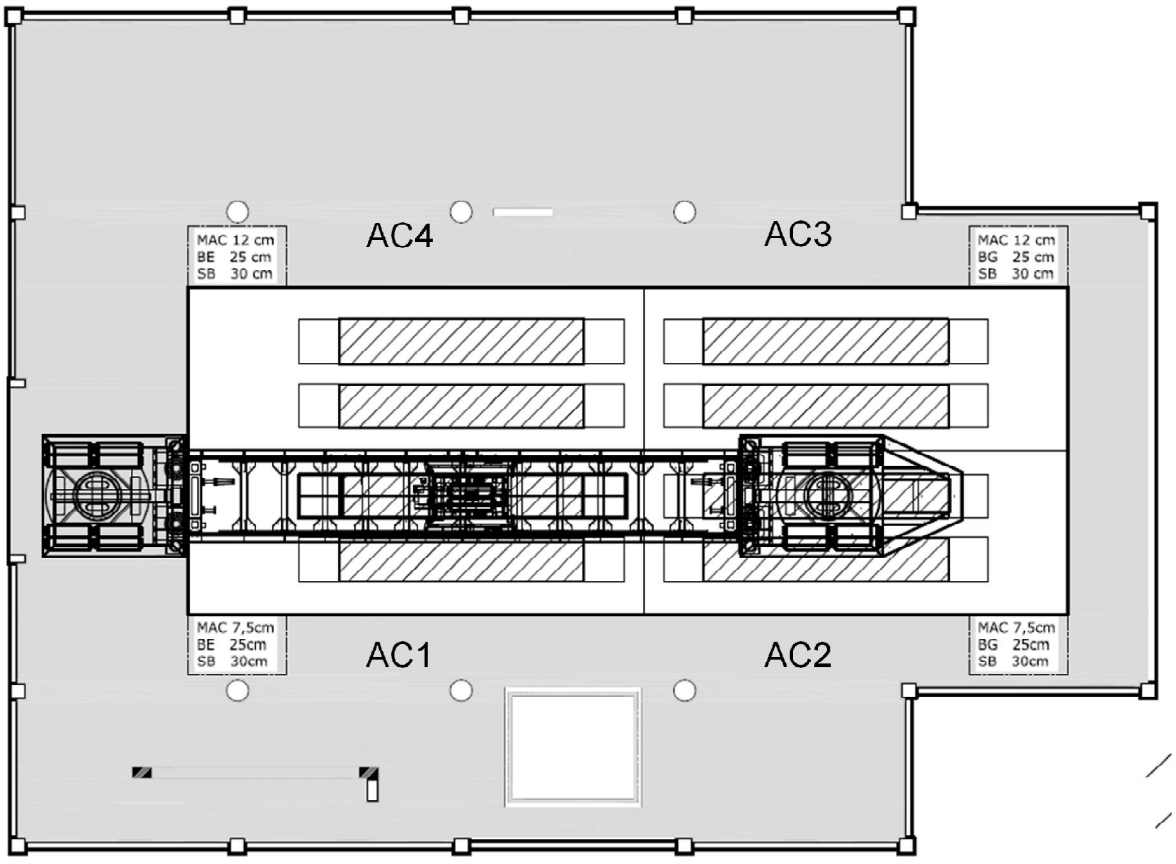

FIGURE 1 Test track distribution.

TABLE 1 Test Tracks in-place Properties

Properties\Section	AC1	AC2	AC3	AC4
H1, cm - (HMA)	5.1	6.3	13.2	13.2
H2, cm - (Base)	21.9	21.2	31.0	24.9
H3, cm - (SB)	30.1	30.1	30.1	30.1
E1 @ 25 °C, MPa	3800	3800	3800	3800
E2, MPa	1200	170	170	1200
E3, MPa	140	140	140	140
E4, MPa	70	70	70	70

Instrumentation

The experiment included not only the instrumentation integrated with the HVS system but also embedded instrumentation in all four test sections. HVS onboard sensors can record the applied load, tire pressure and temperature, position of the load and the velocity of the load carriage. Embedded instrumentation include asphalt strain gauges (PAST sensors), pressure cells (SOPT sensors), multi depth deflectometers (MDD), moisture and temperature probes. These sensors were chosen based on previous HVS owners experience (*9, 10*). Additionally, the HVS was equipped with a laser profiler that can be used to create a tridimensional profile of the section and a Road Surface Deflectometer is added to the testing equipment to obtain deflection basins at any location along the test section.

Figure 2 shows the instrumentation array used for the first series of experimental sections. The PAST sensors were placed at the base/HMA layer interface and were placed in the longitudinal or traffic loading direction and in the transverse direction. MDD sensors were installed at 4 different depths to cover all 4 structural layers. As for the thermocouples, these were placed at 4 depths: surface, middle depth of the HMA layer, at the PAST sensors depth and 5 cm into the base layer. In the case of AC1 and AC3 sections the same gauge array was used while excluding PAST sensors.

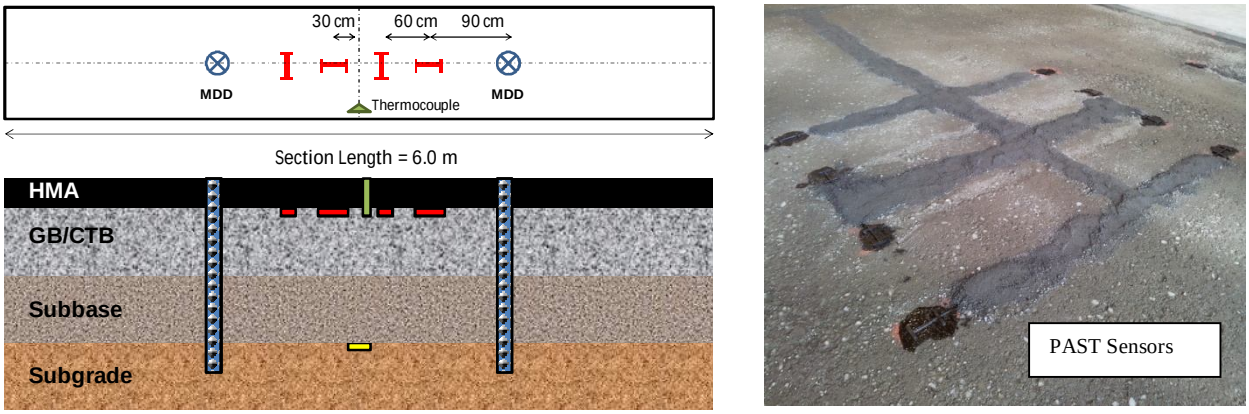

FIGURE 2 Sensor Array.

Data collection of the 3D profile, strain, pressure, temperature and deflection is performed based on load repetitions. At the beginning of the test, data are obtained at short intervals. After 15,000 load repetitions, data are collected on daily basis. Inspection of fatigue and reflective cracking, friction loss,

loss of aggregate-asphalt bond and any other surface damage is performed on daily basis during the HVS daily maintenance work.

RESULTS

Section AC1 was the first evaluated structure in Costa Rica using the HVS. Testing started in mid July 2012 and ended at the beginning of December of 2012. A total of one million load repetitions at four different load levels where applied in bi-directional mode with a set speed of 10 km/h. A wheel wandering of 10 cm was also set for the test. As an indoor facility, temperature was relatively constant throughout the entire test. Ambient and pavement temperature varied from 20 °C to 25 °C. Results of the collected data and analyses are presented as follows:

FWD testing and construction variability

Each constructed section is approximately 10 meters long by 4 m wide. Each section is 8 meters long by 1 m wide. Figure 3 shows the average deflection for a 9 sensor configuration of a Falling Weight Deflectometer with a 40 kN load on the AC1 section. Relatively higher deflections were observed on the extremes of the section indicating lower structural capacity on these areas, and overall it was an indication of construction and materials variability. These higher deflections occurred near the load plate, which are related to the structural condition of the upper layers. This also indicates that the observed heterogeneity in deflections can be attributed to the variability in material properties and thickness variability of the upper layers. Conversely, similar deflections measured in the farthest point from the load plate suggest low variability in the properties of the underlying layers.

In order to validate the previous observations, deflection basin parameters were used to quantify the structural capacity of the different layers. Surface Curvature Index (SCI), Base Curvature Index (BCI), and Base Damage Index (BDI) are also shown on Figure 2. In general, it is stated that high values of these parameters correspond to pavement structures with low support capacity (*11*). The SCI parameter is related to upper layers structural capacity. SCI values greater than 300 µm indicate potential structural weaknesses in the upper layers. BDI values near or greater than 100 µm indicate potential structural deficiencies in the intermediate layers. BCI values near or greater than 80 indicate potential structural defects in the underlying layers. According to the previous classification, there is a deficiency in the middle layers (base, sub-base) within the first 4 meters of the constructed section and in general a weaker structure. On the other hand, the supporting layer showed the lowest variability overall, based on the BCI parameter.

a.

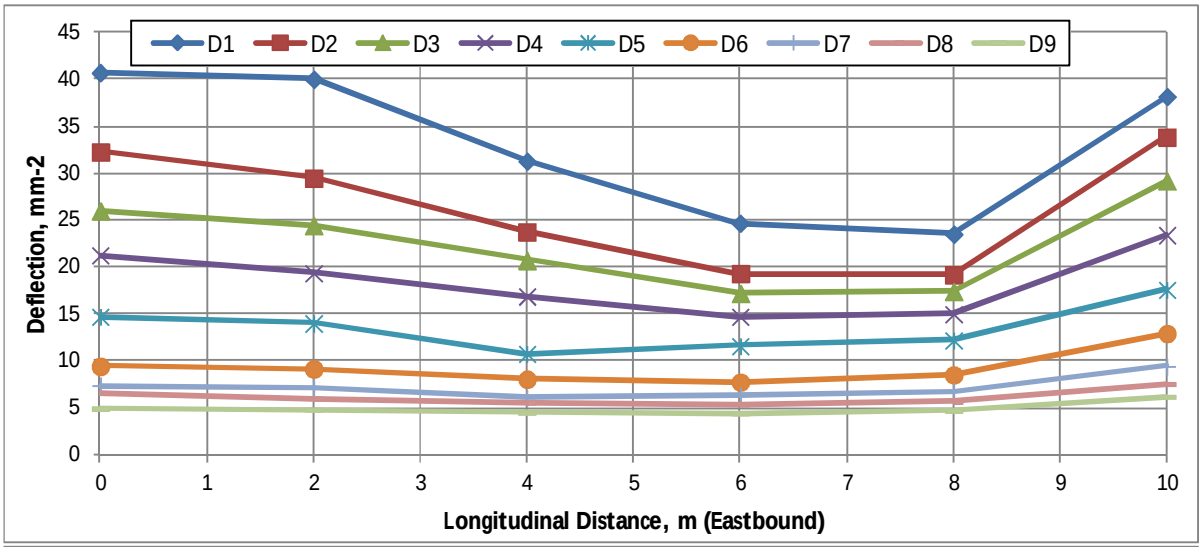

b.

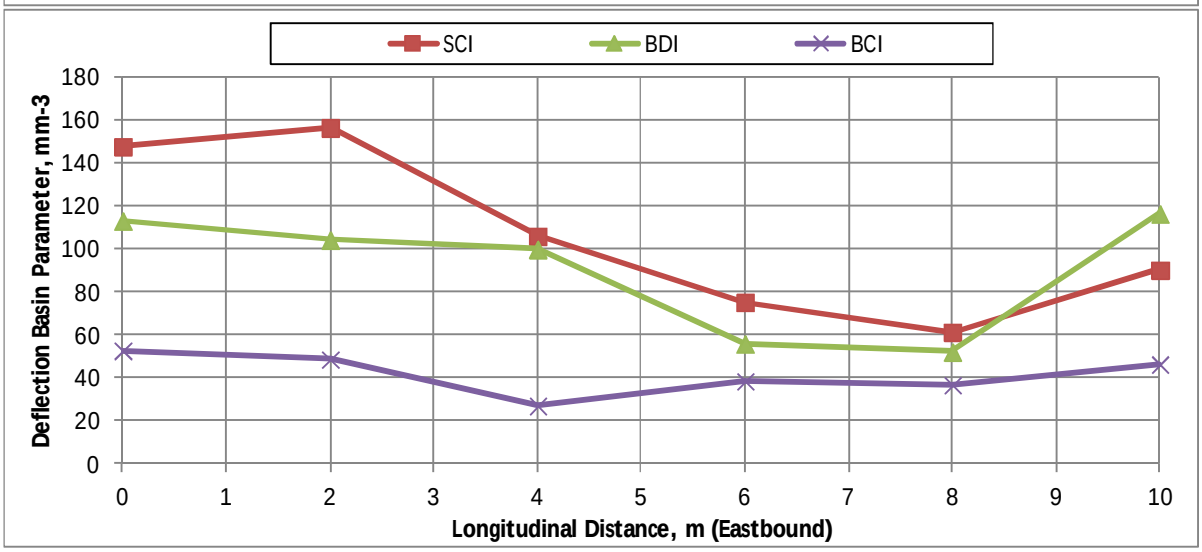

FIGURE 3 FWD tests results a. Deflections @ 40 kN, b. Deflection Basin Parameters.

Determination of the layer thickness of the pavement structure was performed using a Ground Penetrating Radar (GPR) model Geo-GSSI RoadScan with 1 and 2 GHz antennas and a SIR-30 data acquisition system. These results were obtained with a high degree of reliability due to the presence of copper plates placed at the interfaces of various layers. Thicknesses measured on a copper plate are most accurate because the signal is fully reflected therefore easier to locate. Copper is also used for equipment calibration and for estimating the dielectric constant of the materials. Figure 4 shows an image of the GPR test performed over the longitudinal direction of AC1 and AC2 sections along with the computed layer thicknesses for AC1. With the highest variability, the thickness of the HMA layer varied from 4.2 to 6.9 cm with an average of 5.1 cm and a coefficient of variation of 12%. The thickness of the base layer varied from 17.7 to 31.1 cm with an average of 21.9 cm and a COV of 11%. Finally, the thickness of the base layer varied from 24.1 to 39.9 cm with an average of 30.4 cm and a COV of 10%.

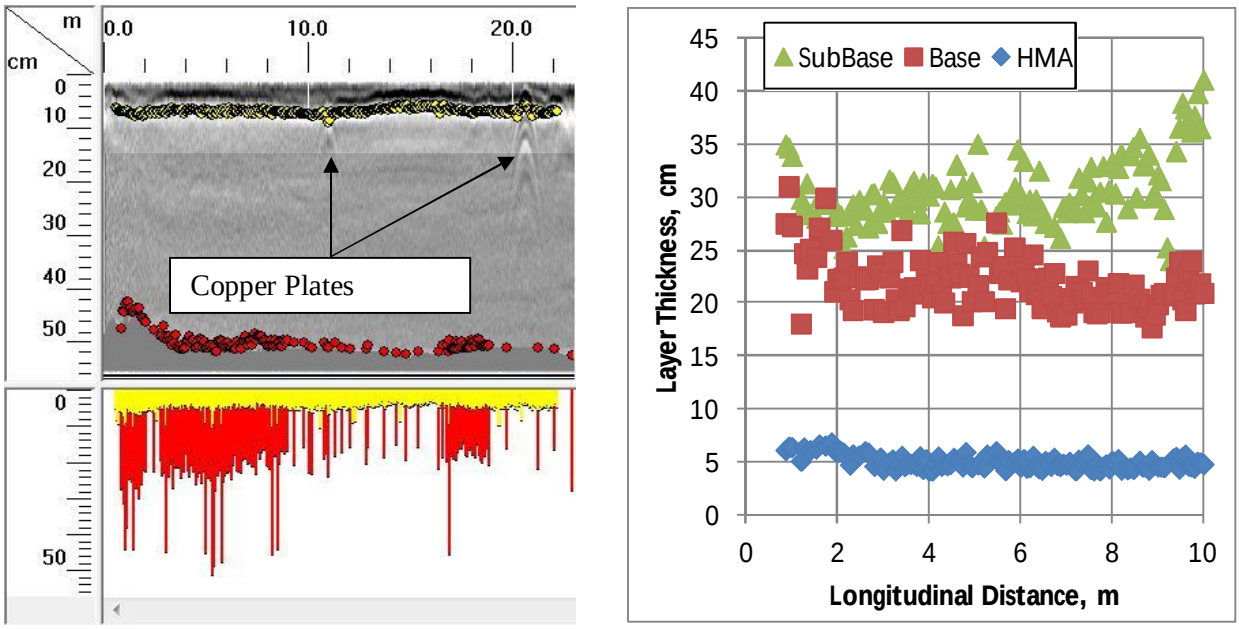

FIGURE 4 Layer Thickness Variability.

Compressive vertical stress at subgrade level

Initially the load was set to 40 kN which corresponds to standard design load. In order to accelerate the damage process the load was increased to 60 kN, 70 kN, and finally 80 kN. Figure 5 shows the load increase at different number of applied repetitions and the effect of the load increment on the subgrade measured stress level. As expected, at each load increment the stress level increased significantly and at a constant load level the stress slightly increased which is evidence of accumulated damage taking place and loss of supporting capacity.

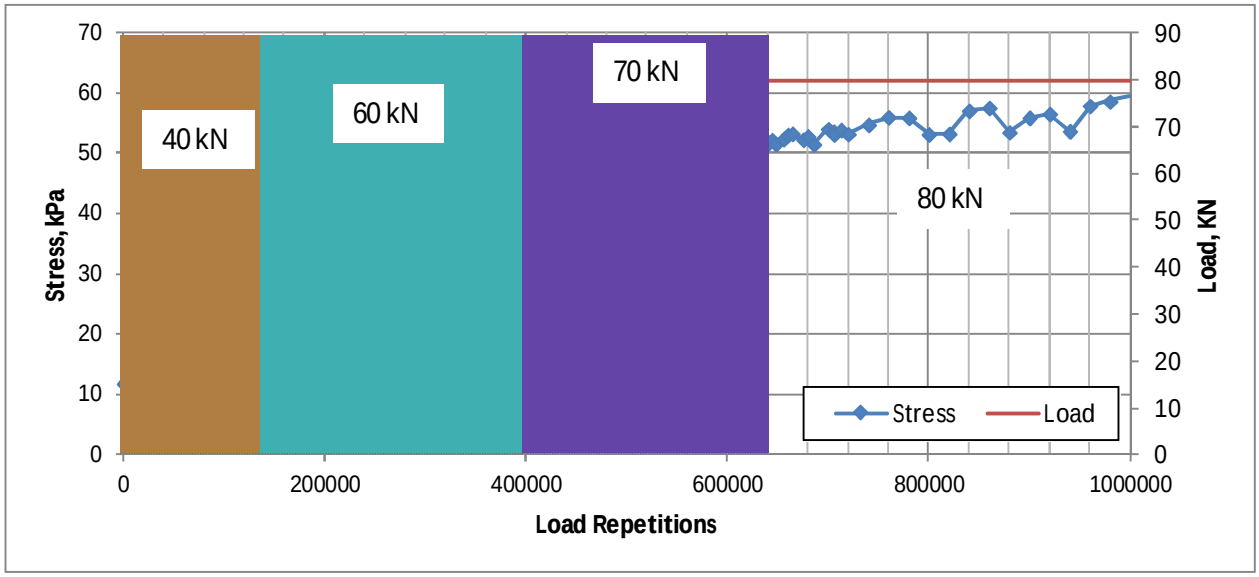

FIGURE 5 Load and compressive vertical stress level.

Profile and Surface Permanent Deformation

Figure 6 shows an example of a 3D profile and the average cross sections obtained from the measured profile at different load levels. The test section 8.15 m long and 1.6 m wide. 1.0 m is required on each extreme as acceleration/deceleration zones for a total of 6.15 m effective test section. Due to the eccentric positioning of the laser with respect to the loading position, an effective length for the surface profile of 5.1 m is obtained. The 3D profile shows that rut depths were higher on the west side of the section which corresponds to the weak area found with FWD testing. On the contrary, lower rut depths were found near the center and east side of the section were the structural capacity was found to be higher. Figure 6 shows that both, consolidation of the pavement structure and the asphalt mixture lateral displacement were obtained. The latter started to occur after around five hundred thousand load repetitions.

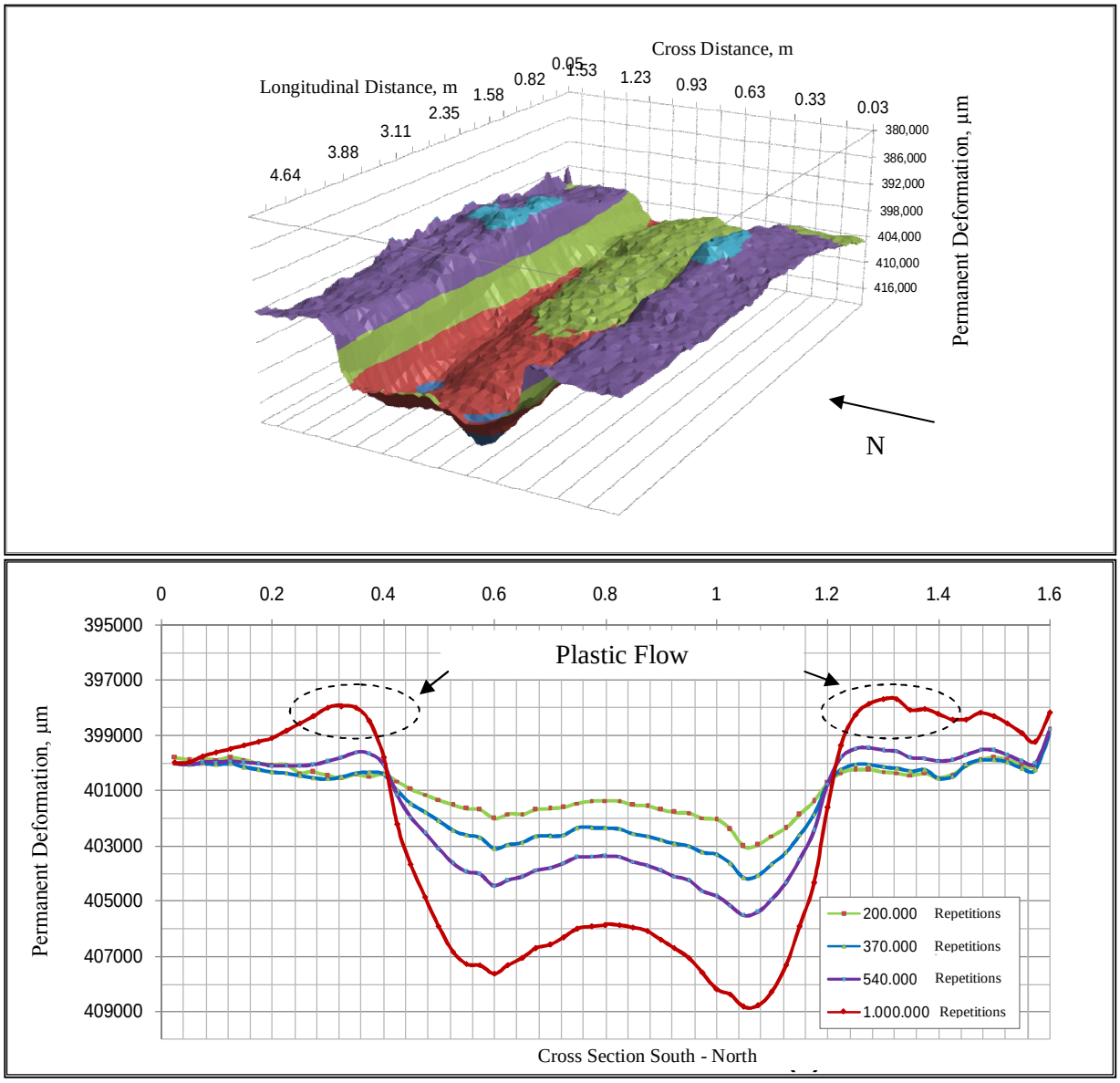

FIGURE 6 3D-Profile and cross section.

Permanent deformation progression due to actual loading and Equivalent 40 kN Load Repetitions can be seen on Figure 7. The figure includes the value of maximum deformation, the minimum deformation and a value representative for the section (reference location selected along the middle third of the section) used to control the daily deformation accumulation and to eventually stop the test upon exceeding the failure criteria. To transform the number of load repetitions at different loading levels to standard loads, it is required to account for a damage factor (Equation 1). The damage factor used to calculate the equivalent 40 kN number of repetitions based on other load levels was 4.2. This value was obtained from previous research using similar equipment (*6*). The test was stopped when the permanent deformation at the reference location reached 12.5 mm. As expected, permanent deformation occurred at a higher rate at the beginning of the test due to insufficient compaction of the HMA layer during construction (primary stage). A secondary stage where rut depth increases at a relatively constant rate was also observed on the section that showed higher structural capacity. The transition to a tertiary stage where the mixture started to flow could be observed on the section that showed lower support capacity.

$$ELR = \left(\frac{P}{40\ kN} \right)^{DF} \times R \qquad \text{Equation 1}$$

where;
ELR = Equivalent 40 kN Load Repetitions
P = Actual Load
DF = Damage Factor (4.2)
R = Number of load repetitions at the actual load

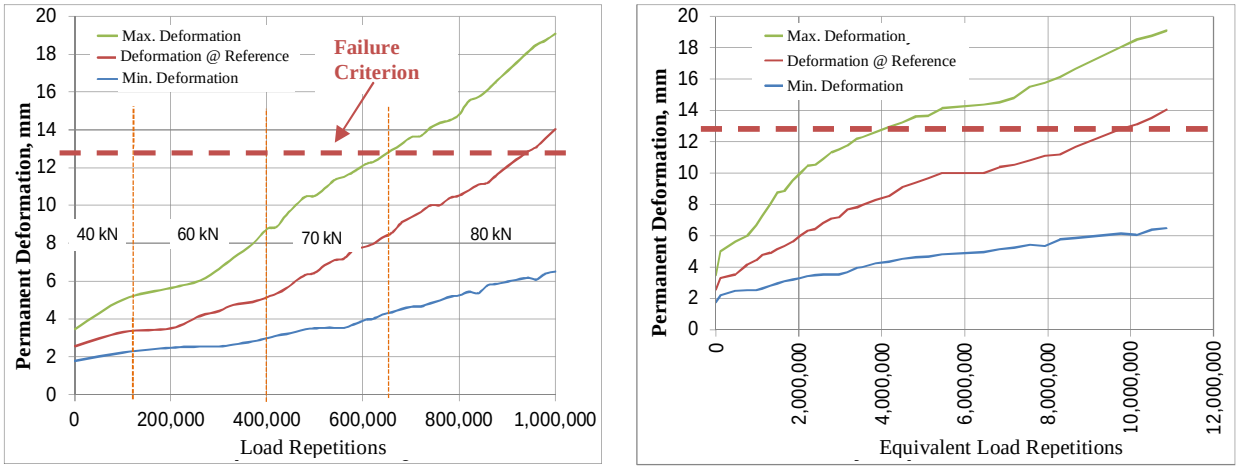

FIGURE 7 Permanent deformation progression.

Roughness

Surface roughness was quantified using the International Roughness Index (IRI) based on longitudinal surface profile readings collected with the built-in laser system. Figure 8 shows the progression of the roughness as function of the applied load repetitions and the respective equivalent load. The initial surface roughness values were close to 1.5, then decreased slightly to 1.3 most likely due to post-compaction. Subsequently with the increase in the load repetitions, the deterioration of profile increased at an approximate rate of 0.06 mm/m/10^6 equivalent loads. It should be noted that the previous IRI values are limited to the length of the test section.

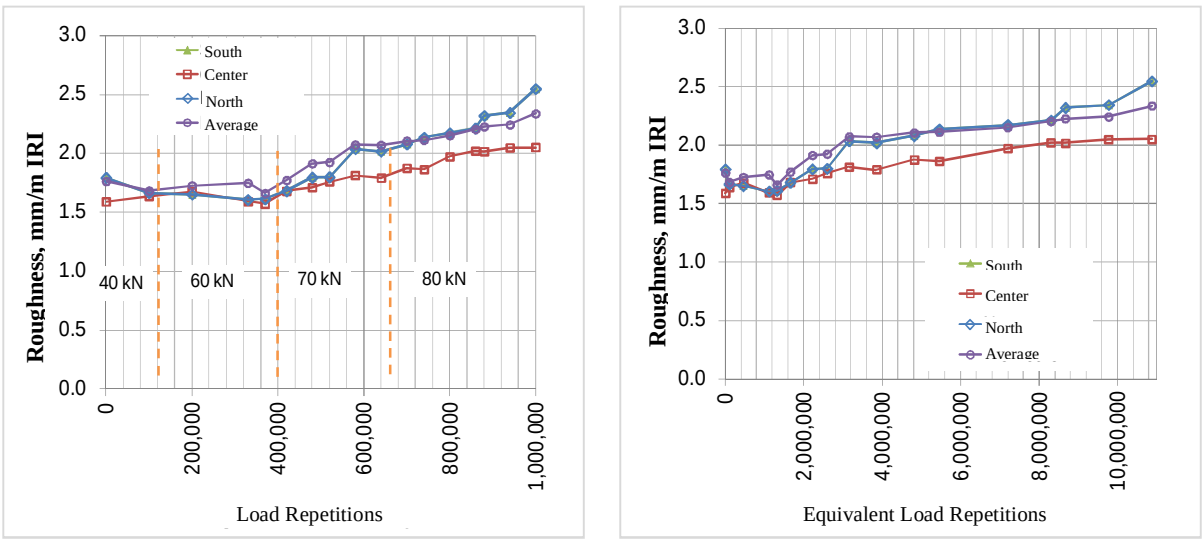

FIGURE 8 Roughness (IRI) Progression.

Multiple depth deflections and deformations

The evolution of the instantaneous elastic deflection and permanent deformation for all four layers during the test are shown on Figure 9. These values were obtained for a 40 kN load. As in the case of vertical pressure, evidence of cumulative damage was observed since an increase in the level of instantaneous deflection was obtained for a relatively constant temperature and test load. The accumulation of damage was observed for all of the layers; however, the upper layers exhibited the largest change. In terms of permanent deformation it was observed that the MDD sensor placed on the surface (mdd1-0) showed the highest deformation (5.3 mm), while the other sensors reported similar deformation (between 1.5 and 1.9 mm). This indicates that the asphalt mixture is responsible for most of the plastic deformation. The deformation below the HMA layer can be expected to be constant because of the capacity of the CTB layer.

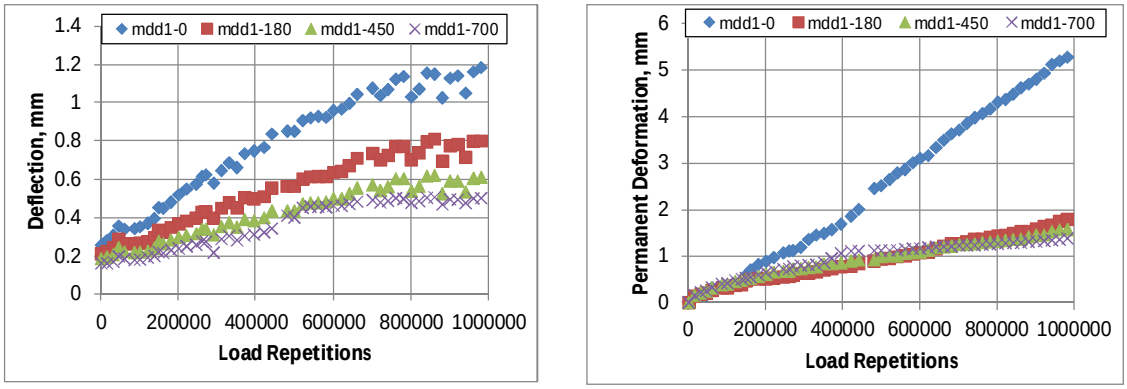

FIGURE 9 Progression of deflection and deformation obtained from MDD sensors.

The Road Surface Deflectometer (RSD) was used to measure deflections at other locations along the section. Figure 10 shows the progression of the maximum deflection at 4 different points located near the ends of the section. The accumulated damage was found to be greater towards the western end of the section which coincides with high deflections measured with the FWD.

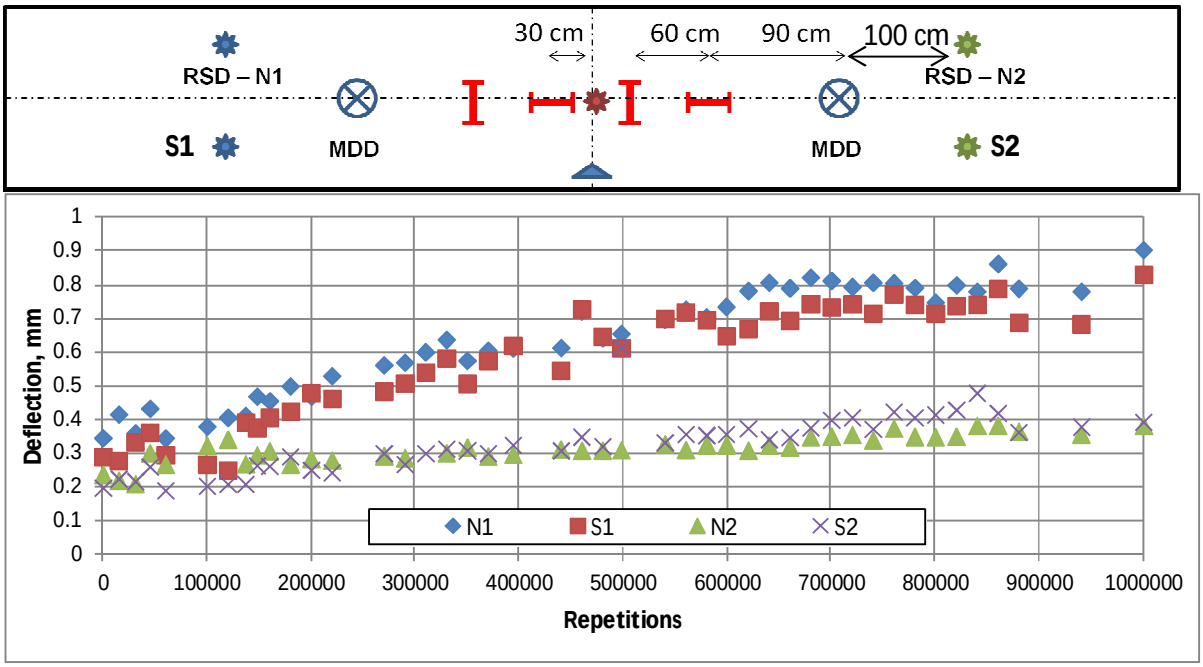

FIGURE 10 Progression of deflection RSD testing.

Deflection Analysis

Deflection basins were obtained before and after loading based on 3 different sources: FWD, RSD and MDD. The RSD and MDD surface deflections were measured in the previously defined locations, based on a wheel load traveling at 7.6 mph. The FWD deflections were obtained from the standard impact load. The results of the measured deflections and their respective surface modulus are shown on Figure 11. At the beginning of the test, all 3 deflection basins were similar with slightly higher FWD deflections. An analysis of deflection basins using surface modulus theory indicated that FWD results most likely reflect an elastic linear behavior of the lower layers while RSD and MDD reflect a moderately non-linear elastic behavior (*11*). Furthermore, higher surface moduli near the center of the applied load suggests higher supporting capacity of the upper layers (higher moduli).

Significantly lower deflections near the center of the applied load were obtained at the end of the test. These results are also shown on Figure 11. A similar surface modulus analysis indicated that FWD results consistently reflect an elastic linear behavior of the lower layers, while RSD and MDD reflect a more intensified non-linear behavior of the lowers layers and could also exhibit the presence of a shallow rigid layer or bedrock. Moreover, lower surface moduli near the center of the applied load suggests a significant decrease of the supporting capacity of the upper layers.

a.

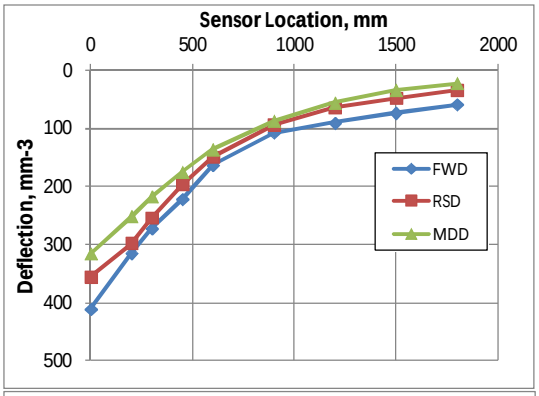

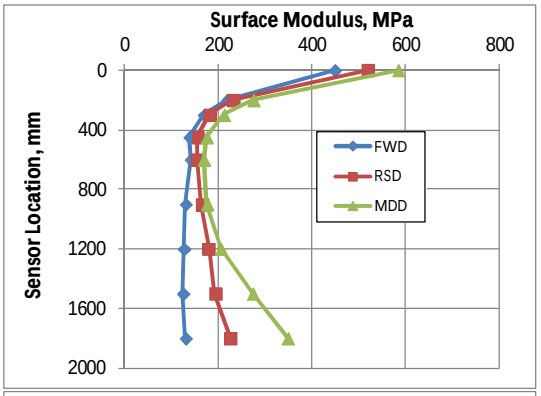

b.

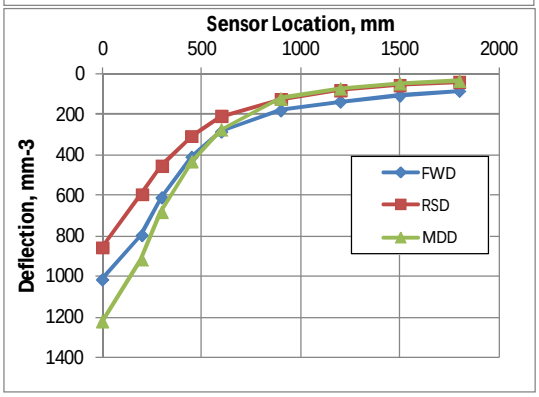

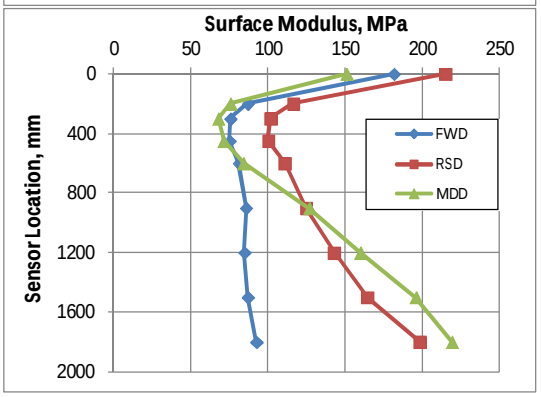

FIGURE 11 Deflection comparison a. Before, b. After loading.

Backcalculated Layer Moduli

Estimated layer moduli based on FWD test results were first shown in Table 1 for the initial pavement condition. At the end of the test the backcalculated layer moduli exhibited a significant decrease for the cement treated base as expected. The average modulus for the CTB layer was 250 MPa, 79% lower than the initial result (1200 MPa). The asphalt concrete layer had a modulus decrease of 30% while the granular base and subgrade moduli were 15% and 22% respectively.

MDD deflection data were used to determine the progression of the pavement layer moduli. This was done by applying the method of equivalent thickness (*11*) whereby the thickness of the structure is transformed into a single layer. This transformation is done using Odemark´s methodology (Equation 1) and calculation of stresses, strains and deflections were performed using Boussinesq theory. For the determination of subgrade modulus, the nonlinearity was considered using the regression coefficients shown in Equation 2.

Figure 12 shows the backcalculated layer moduli for the HMA, CTB and sub-base layers, as well as the estimated "C" value (from Equation 2) for the subgrade. The estimated "n" coefficient was on average -0.40. Figure 11 shows that the CTB layer had the highest decrease in modulus followed by the HMA layer. Conversely, no significant change was found for the sub-base modulus. A decrease in the subgrade non-linear coefficient "C" is also an indication of a decrease in the layer modulus. Finally, measured and estimated deflections were compared to show the effectiveness of the backcalculation procedure. A good correlation obtained between measured and estimated deflections and a small deviation from the equality indicated that the backcalculation methodology can be successfully applied to this particular data set.

$$h_{e,n} = f \cdot \sum_{i=1}^{n-1}\left(h_i \cdot \sqrt[3]{\frac{E_i}{E_n}} \right) = f\left\{ \left[\left(h_1 \cdot \sqrt[3]{\frac{E_1}{E_2} + h_2} \right) \cdot \sqrt[3]{\frac{E_2}{E_3}} \right] \cdot \ldots h_{n-1} \right\} \cdot \sqrt[3]{\frac{E_{n-1}}{E_n}} \quad \text{Eq. 1}$$

Where,
E_i = Layer modulus
h_i = layer thickness
f = correction factor

$$E_{SR} = C \times \left(\frac{\sigma_d}{0.1MPa} \right)^n \quad \text{Eq. 2}$$

Where,
E_{SR} = Subgrade Modulus
σ_d = Deviator stress
C y n = regression coefficients

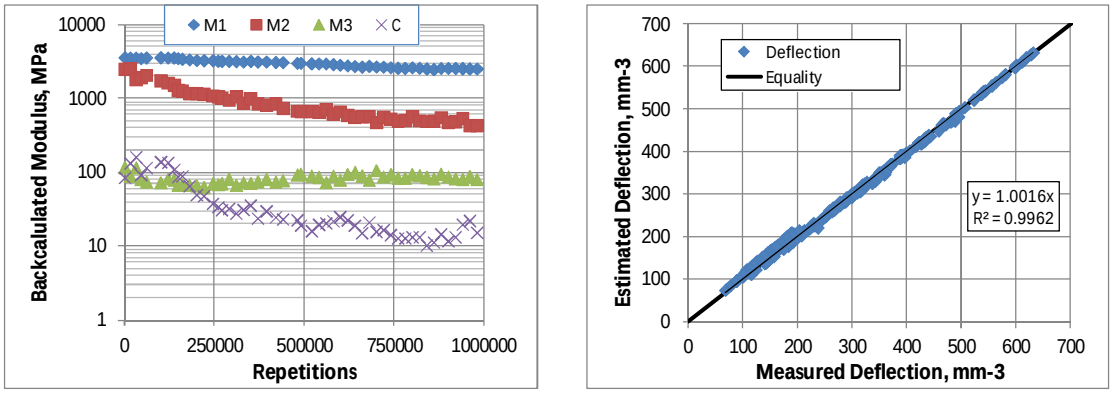

FIGURE 12 MDD Backcalculated Layer moduli.

Mechanistic-Empirical Modeling

The HVS carriage dual-tire configuration with a total load of 40 kN (20 kN per tire) was modeled using *3D-Move Analysis_V2*. This software includes pavement performance models that predict pavement distresses such as fatigue cracking and rutting that were obtained from the NCHRP 1-37A study. The tool accounts for moving traffic loads with complex contact stress distributions of any shape, vehicle speed, and viscoelastic properties of asphalt concrete layers to calculate pavement responses using a continuum-based finite-layer approach. A dynamic analysis was performed using viscoelastic properties for the HMA layer obtained from dynamic modulus test results. For the remaining materials, only a linear elastic behavior can be modeled and the respective layer moduli are shown on Table 1. The dynamic modulus master curve is shown on Equation 3 . The laboratory results were obtained following AASHTO TP 79-11.

Table 2 shows the modeled structure and the expected performance after 10 million 40 kN dual-tire load repetitions. A small amount of cracking was predicted for this section, however, at the end of the accelerated test this type of distress was not observed within the effective test section. Regarding the rutting target level, the HMA layer did not meet the limit criteria. Nevertheless, the predicted HMA rutting was the closest one to the actual value (2.7% difference). On the other hand, rutting performance of the remaining layers were slightly underestimated. Moreover, the total rut depth was 10.3 mm which was 17.6% below the actual value.

Overall, there predicted performance followed the observed trend of the actual results with regards to rutting. The highest rut depth was obtained and predicted for the top layer and significantly lower

permanent deformation was measured for the bottom layers. Further investigation with other APT sections may confirm the applicability throughout local calibration of the NCHRP 1-37A performance models.

$$\log|E^*| = 0.1787 + \frac{3.526}{1 + e^{-1.444 + -0.5139\left\{\log\omega + \frac{197674}{19.14714}\left[\left(\frac{1}{T}\right) - \left(\frac{1}{T_r}\right)\right]\right\}}} \qquad \text{Eq. 3}$$

Where,
E* = dynamic modulus, ksi
ω = frequency, Hz
T = Analysis temperature (296.15 K)
Tr = Reference temperature (294.15 K)

TABLE 2 Modeled Performance

Layer	Distress Type	Distress Target	Reliability Target	Distress Predicted	Reliability Predicted	Acceptable	Actual Result
Asphalt (1)	AC Top Down Cracking (m/km)	190	90	0.47	100	Pass	Non visible
	AC Bottom UP Cracking (%)	25	90	4.81	100	Pass	Non visible
	AC Rutting (mm)	6.4	90	7.4	32.1	Fail	7.2
Base (2)	Base Rutting (mm)	7.6	90	0.8	100	Pass	1.9
Subbase (3)	Subbase Rutting (mm)	6.4	90	1.3	100	Pass	1.8
Subgrade (4)	Subgrade Rutting (mm)	5.1	90	0.8	100	Pass	1.6

CONCLUSIONS

This paper shows an overview of the implementation and results of the first accelerated pavement test in Costa Rica. Based on the experimental results it can be concluded that:

- Construction and material variability have an important effect on the overall performance of a pavement structure. FWD testing results indicated that the section could have weak spots especially to the west side. Permanent deformation patterns coincide with the structural capacity and variability found along the section.
- Embedded instrumentation has proved to be an efficient tool to monitor the behavior and performance over the life span of pavement structures. In this case, the amount and quality of information obtained from the MDD sensors confirmed expected trends for the type of the evaluated structure.
- The information obtained from accelerated testing can be used to calibrate and / or validate input parameters required in new and increasingly popular mechanistic pavement design methodologies.

REFERENCES

1. LTPP. *LTPP Beyond FY 2009: What Needs to Be Done*?. Report FHWA-HRT-09-052. 2009.

2. Metcalf, J. B. *NCHRP Synthesis of Highway Practice 235*. 1996.

3. Coetzee, N et al. *The Heavy Vehicle Simulator in Accelerated Pavement Testing: Historical Overview and New Developments*. 3rd International Conference APT. 2008.

4. Harvey, J. T., Hoover, T., Coetzee, N. F., Nokes, W. A., and Rust, F. C. *Caltrans Accelerated Pavement Test (CAL/APT) Program—Test Results: 1994–1997*. AAPT Symposiumon Accelerated Pavement Testing, Boston, MA, March 16-18, 1998.

5. Leiva, Aguiar y Loría. *Ensayos Acelerados De Pavimentos En Costa Rica*. Revista Infraestructura Vial, Vol 15 (#26), 33-41. San José Costa Rica, 2013.

6. Harvey, J. T., L. du Plessis, F. Long, S. Shatnawi, C. Scheffy, B-W. Tsai, I. Guada, D. Hung, N. Coetzee, M. Reimer, and C. L. Monismith. *Initial CAL/APT Program: Site Information, Test Pavement Construction, Pavement Materials Characterizations, Initial CAL/APT Test Results, and Performance Estimates.* Report prepared for the California Department of Transportation. Report No. RTA-65W485-3. Pavement Research Center, CAL/APT Program, Institute of Transportation Studies, University of California Berkeley. 1996.

7. Timm, D. NCAT Report 09-01 *Design, Construction And Instrumentation Of The 2006 Test Track Structural Study*, NCAT. 2009.

8. Leiva-Villacorta, F. and D. Timm, *Analysis of Measured Versus Predicted Critical Pavement Strain Responses*, Proceedings of the 90th Annual Transportation Research Board, Washington, D.C. 2011.

9. Heavy Vehicle Simulator. *Monitoring of test sections and instrumentation*. Documento consultado el 6 de abril del 2010. http://www.gautrans-hvs.co.za/}

10. Baker Harris B., Buth Michael R., Van Deusen David A. Minnesota Road Research Project: *Load response Instrumentation Installation and Testing Procedures*. Minnesota Department of Transportation. 1994.

11. Ullidtz, P., *Pavement Analysis, Development in Civil Engineering*, Vol.19, Amsterdam, the Netherlands. 1987.